

Singlet Oxygen Plays an Essential Role in the Root's Response to Osmotic Stress^{1[OPEN]}

Tomer Chen² and Robert Fluhr³

Plant and Environmental Sciences, Weizmann Institute of Science, Rehovot 76100, Israel

ORCID IDs: 0000-0001-9320-0009 (T.C.); 0000-0001-5641-1472 (R.F.)

The high osmotic potentials in plants subjected to drought stress can be mimicked by the application of high molecular weight polyethylene glycol. Here, we quantified the effects of exposure to polyethylene glycol on the growth of the main and lateral roots of *Arabidopsis* (*Arabidopsis thaliana*) seedlings. The effects on root growth were highly correlated with the appearance of singlet oxygen, as visualized using the singlet oxygen-specific probe singlet oxygen sensor green. The production of singlet oxygen was followed by cell death, as indicated by the intracellular accumulation of propidium iodide due to the loss of membrane integrity. Cell death began in the epidermal region of the root tip and spread in a dynamic manner to meristematic sections. In parallel, gene expression changes specific to the presence of singlet oxygen were observed. The accumulation of other reactive oxygen species, namely hydrogen peroxide, nitric oxide, and superoxide, did not correlate with cell death. In addition, both the singlet oxygen scavenger His and the lipoxygenase inhibitor salicylhydroxamic acid specifically inhibited singlet oxygen accumulation and cell death. These results suggest a light-independent, type-I source of singlet oxygen production. Serpin-protease interactions were used as a model to assess the possibility of vacuolar-type cell death. Osmotic stress induced the accumulation of complexes between the cytoplasmic serpin AtSERPIN1 and its cognate vacuolar proteases, indicating that vacuolar integrity was compromised. These findings imply that singlet oxygen plays an essential role in conveying the root response to osmotic stress.

Drought is a common adverse environmental factor that affects plant water balance, eliciting multiple reactions in the plant that severely limit plant productivity (Godfray et al., 2010). The altered soil-water status has a profound effect on lateral root initiation and elongation (van der Weele et al., 2000; Deak and Malamy, 2005). Experimental systems to understand the effects of drought have incorporated cell-impermeable high molecular weight polyethylene glycol (PEG; Lagerwerff et al., 1961; Verslues et al., 1998). The use of PEG showed that drought stress response could be separated into components of high osmotic pressure effects and of high salt toxicity effects, with each exhibiting distinct transcriptome profiles (Patade et al., 2012; Monetti et al., 2014). Indeed, PEG-generated osmotic stress was used to select for novel drought-resistant rice genotypes in embryogenic calli. The regenerated lines were shown

to have elevated Pro content (Joshi et al., 2011), where Pro imparts both osmolyte protection and antioxidative properties (Hayat et al., 2012). Thus, PEG-induced stress is a useful experimental system for studying drought response.

Drought stress has been well documented in the leaf to be associated with a variety of reactive oxygen species (ROS). For example, due to the decrease in leaf stomatal conductance, CO₂ availability during drought is limited, leading to increased photorespiration (Voss et al., 2013). This can result in increased toxic singlet oxygen production in the chloroplast (Gechev et al., 2012). Furthermore, photoinhibitory conditions in the chloroplast stimulated by drought and high light were shown to promote multiple types of ROS due to reduced chloroplast-scavenging capabilities (Petrov et al., 2015; Feller, 2016). Perturbation of mitochondrial electron transport in drought also contributes to ROS production (Rhoads et al., 2006). In that case, modification of mitochondrial alternative oxidase, an activity that regulates the organelle redox state, was shown to ameliorate drought sensitivity (Giraud et al., 2008). The levels of ROS were shown to be controlled at the transcription level by transcription factors. For example, the *ntl4* mutant, defective in a stress-responsive NAC transcription factor, exhibited lower ROS, delayed leaf senescence, and enhanced drought resistance (Lee et al., 2012; Takasaki et al., 2015).

The effects of osmotic stress and resultant ROS are well characterized in the aerial portions of the plant, but less is known about the manifestations of drought-induced ROS and programmed cell death (PCD) in the root. In *Arabidopsis* (*Arabidopsis thaliana*),

¹This work was supported by the I-CORE Program of the Planning and Budgeting Committee and the Israel Science Foundation (grant nos. 757/12 and 1596/15) and as part of the ISF-UGC joint program (grant no. 2716/16).

²Current address: Department of Plant Sciences, Weizmann Institute of Science, P.O. Box 26, Rehovot 76100, Israel.

³Address correspondence to robert.fluhr@weizmann.ac.il.

The author responsible for distribution of materials integral to the findings presented in this article in accordance with the policy described in the Instructions for Authors (www.plantphysiol.org) is: Robert Fluhr (robert.fluhr@weizmann.ac.il).

T.C. carried out the experimental work; T.C. and R.F. formulated the hypotheses and wrote the manuscript.

^[OPEN]Articles can be viewed without a subscription.

www.plantphysiol.org/cgi/doi/10.1104/pp.18.00634

PEG-induced dehydration led to hydrogen peroxide production in the root tip, as measured by general non-specific probes for ROS, namely 3,3'-diaminobenzidine and 2',7'-dichlorofluorescein (Duan et al., 2010). In that case, ROS production was accompanied by organelle degradation. However, other experiments showed a greater difference in the root transcriptome analysis of hydrogen peroxide-induced genes during salt stress compared to osmotic stress (Miller et al., 2010). Thus, there is a need to further characterize ROS response to stress induced by osmotic stress in roots.

Bioinformatics analyses of multiple stresses in leaves, including drought, demonstrated signatures of singlet oxygen in both dark and light conditions (Rosenwasser et al., 2013). The singlet oxygen sensor green (SOSG) probe, a specific two-component trap-fluorophore system, is activated by singlet oxygen (Flors et al., 2006; Gollmer et al., 2011). Consistent with the appearance of singlet oxygen transcriptome signatures, an increase in SOSG fluorescence was detected in the dark during biotic and abiotic stresses in root tips (Mor et al., 2014). Similarly, drought simulation by dehydration treatment of leaves led to the rapid generation of singlet oxygen as quantified by radical formation in the singlet oxygen-specific spin trap 4-hydroxy-tetramethylpiperidine (Koh et al., 2016). Thus, singlet oxygen can have nonphotosynthetic origins; however, the role of such "dark" singlet oxygen in determining the milieu of plant responses to stress is obscure. As the root lacks photosynthesis, it is the ideal organ in which to study nonphotosynthetic sources of singlet oxygen.

Osmotic stress responses in the root include PCD (Duan et al., 2010). PCD is one means by which plants can remobilize essential nutrients to benefit surviving tissue (Munne-Bosch and Alegre, 2004; Rogers and Munné-Bosch, 2016). In the root tip, PCD can be viewed as an adaptive mechanism promoting lateral root development (Huh et al., 2002; Ji et al., 2014). Mechanistically, PCD can be orchestrated by the disruption of the tonoplast, as shown to occur during acute dehydration stress in leaves (Koh et al., 2016). Indeed, in roots, osmotic stress was shown to result in general organelle membrane and vacuolar disruption, as qualitatively visualized by electron microscopy (Duan et al., 2010). The vacuoles harbor proteases that play an essential role in vacuolar-mediated cell death during pathogenesis (Hara-Nishimura and Hatsugai, 2011; Dickman and Fluhr, 2013). Upon disruption of the tonoplast, cell death Cys proteases are released and their activity is modulated in the cytoplasm by the presence of serpin protease inhibitors that form inhibitory covalent complexes (Lampl et al., 2010, 2013). However, whether this process occurs in roots during cell death that is initiated by osmotic stress is unknown.

In this work, we chose *Arabidopsis* as a model to analyze cell death induced by osmotic stress. Our findings show that singlet oxygen, as reported by SOSG, appears rapidly in the epidermal cell region of the root and spreads in a dynamic manner to other sections of the root. The resultant dynamics of cell death, as

measured by plasmalemma membrane integrity, follow the appearance of singlet oxygen, but not of other ROS. Furthermore, singlet oxygen-responsive transcripts are induced. The appearance of singlet oxygen and the accompanying cell death were inhibited by His, a singlet oxygen scavenger, and by salicylhydroxamic acid (SHAM), an inhibitor of lipoxygenases. The latter result suggests a light-independent, type I source for singlet oxygen accumulation. Other ROS were not affected by such treatments. Finally, osmotic stress is shown to compromise vacuolar integrity, as indicated by the formation of covalent serpin-protease complexes.

RESULTS

Osmotic Stress Diminishes Root Elongation and Induces Cell Death

Growth rate as a function of the length of PEG treatment was measured in 7-d-old roots. Seedlings were transferred to PEG (30%; -2.035 MPa) for different durations and then returned to regular growth media for measuring growth rate over a 5-d period (Supplemental Fig. S1). Root growth rate was progressively inhibited over 4 to 8 h of PEG treatment, and the main root ceased to grow after 8 h (Fig. 1A). Interestingly, roots that were exposed to PEG treatments of 4 to 8 h and then grown further in regular media showed a local spot of "scarring" in the differentiation zone, as indicated by tissue that lacked root hairs (Supplemental Fig. S2). The observation suggests that intermediate levels of PEG treatment induced cell death in outer-layer cells that are critical for the latter initiation of root hairs. Reciprocally, and concomitant with the decrease in growth of the main root, the subsequent overall length of total lateral roots increased (Fig. 1B). It is known that initiation of lateral roots can be stimulated by direct excision of the main apical tip. The results suggest that more extended PEG treatment also triggered root apical meristematic cell death.

To examine the relationship between death, cessation of growth, and PEG treatment at the cellular level in a dynamic manner, we used propidium iodide (PI) staining to differentiate between live and dead cells. Live cells were impermeable to the stain, and PI was restricted to the cell wall. However, in dead cells, PI permeated the cell and stained the nuclei as well (Supplemental Fig. S3A). To confirm the ability of PI staining to differentiate between live and dead cells, the cell viability stain Sytox green was employed. A high correlation was noted between the two methods of cell viability staining (Mander's overlap = 0.9; Supplemental Fig. S4). When the tissue distribution of the differential staining by PI was examined in PEG-treated roots, the percentage of dead cells increased over a 4-h period, starting from the epidermal cell layer of the elongation zone and progressing to occupy most of the epidermal layer (Fig. 2). In all, cell death initiated by the transient

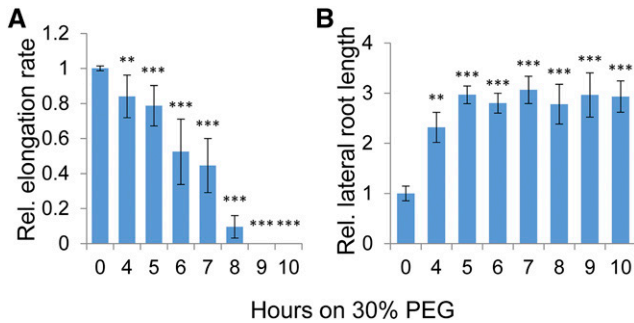


Figure 1. Change in relative root elongation after treatment with 30% PEG. Seedlings were treated with PEG and then plated on Murashige and Skoog plates with 1% Suc. Growth of the main root or adventitious root was measured daily after PEG treatment and quantitated with Fiji software, where no treatment was defined as 1. A, Quantitation of the main root growth rate relative to untreated control, following various PEG treatments. B, Quantitation of the lateral root length relative to untreated control, following various PEG treatments. Error bars are se and $n \geq 9$ seedlings. Asterisks indicate significant difference from the untreated sample (Student's t test, * $P < 0.05$, ** $P < 0.01$, *** $P < 0.001$).

osmotic stress used here was limited to the root distal tip regions that include the apical meristem, basal meristem, and the elongation zone (Supplemental Fig. S3B). In parallel, the roots were labeled with the specific SOSG probe. As shown in Figure 2, the appearance of SOSG fluorescence coincided with latter appearance of cell death (note arrows). The initial fluorescence of SOSG in live cells was generally intense and accumulated in the cytoplasmic regions, whereas a more lingering fluorescence in cells that are permeable to PI appeared to be punctate and weaker and to spread throughout the cell (Supplemental Fig. S5). To quantify this measurement, the area of the root tip with SOSG fluorescence or PI-determined cell death was quantified as shown in the columns on the left (Fig. 2). Thus, the appearance of singlet oxygen as probed by SOSG fluorescence both preceded cell death and persisted after the tissue died as a necrotic postmortem phenomenon (Fig. 2; Supplemental Fig. S5).

To directly assess the viability of cells in the apical meristematic regions after PEG treatment, the integrity of root tissue was measured in a transgenic plant line,

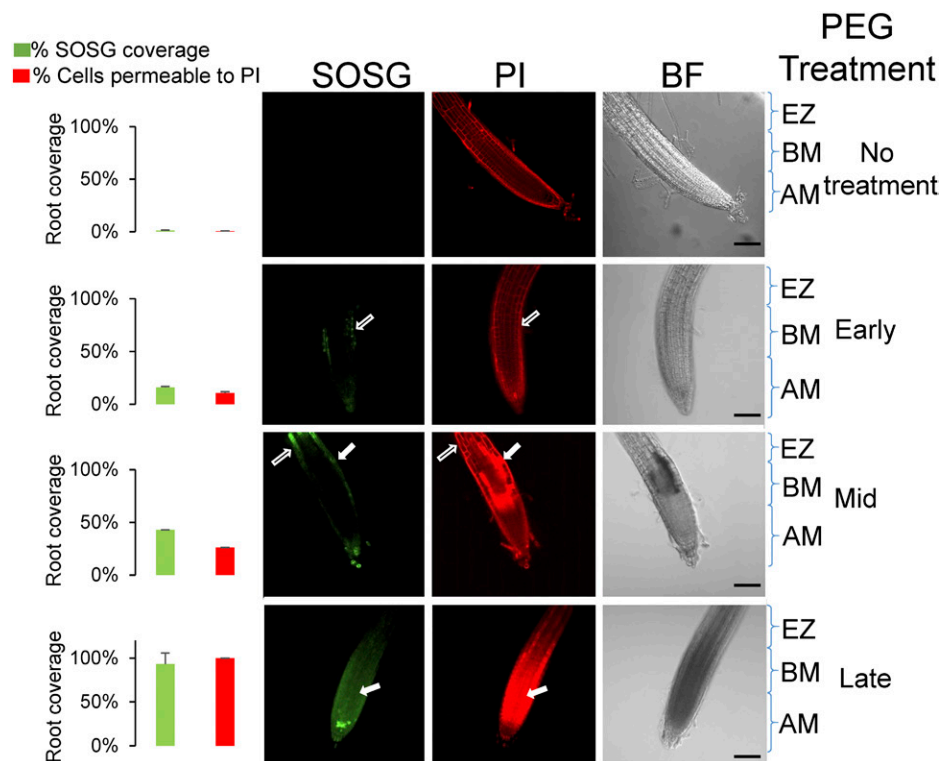


Figure 2. Appearance of singlet oxygen and changes in cell permeability to propidium iodide after PEG treatment. Root tips of 7-d-old seedlings stained with propidium iodide (PI) and singlet oxygen sensor green (SOSG). Median confocal slices are shown for each of these stains, along with the corresponding bright field (BF) image. Treatments were for the times indicated on the right: no treatment; 1 to 2 h, early; 3 to 4 h, mid; 5 to 8 h, late. Zones are as follows: AM, apical meristem; BM, basal meristem; and EZ, elongation zone. The median plane of the root was imaged where opaque regions in PI staining are indicative of cell death. White outlined arrows indicate SOSG and PI staining of live cells (i.e. the stain is observed in the perimeter of the cell). Solid white arrows indicate SOSG and PI staining of dead cells (i.e. where the PI stain permeates and fills the cell). Graphs on the left show quantification of the fluorescence, calculated by estimating the area of the root (using threshold above background) in a median slice that displayed SOSG or opaque PI fluorescence (using threshold above that obtained from live cells). Scale bar, 100 μ m. For quantification, error bars are se , $n \geq 8$.

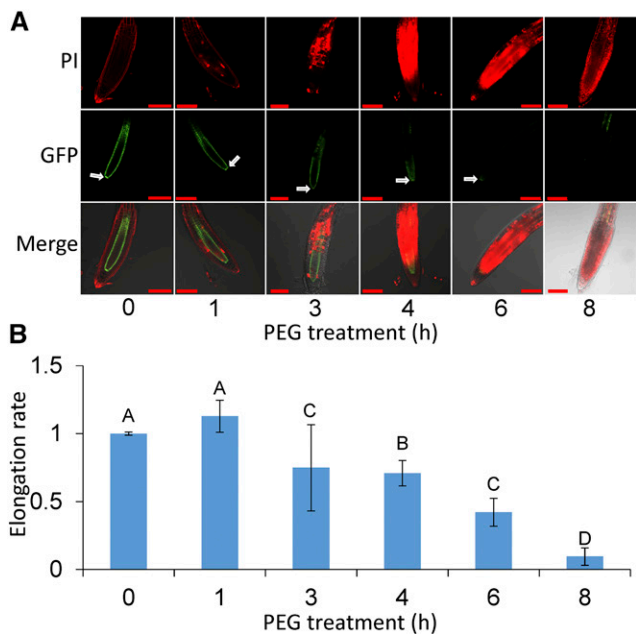


Figure 3. Relationship between integrity of the quiescent center and root elongation. A, Fluorescence resulting from SCR::GFP expression in the endodermis and quiescent center. Roots were exposed to 30% PEG for 1 to 8 h and counterstained with propidium iodide (PI). The median plane was imaged where opaque regions in PI staining indicate cell death. Arrows indicate the quiescent center; scale bars, 100 μ m. B, Root elongation rate following exposure to PEG. Student's *t* test, $\alpha = 0.05$; difference in letters signifies a $P < 0.05$ significant difference; error bars are SE, $n \geq 13$.

where the scarecrow promoter drives GFP expression (SCR::GFP; Sabatini et al., 2003). The roots were counterstained with PI to examine cell viability. Early in the treatment, roots of SCR::GFP displayed fluorescence in the endodermal and quiescent center (Fig. 3; 1 h). As tissue death progressed (4–6 h), the fluorescence signal faded, and at 6 to 8 h of PEG treatment, the cells around the quiescent center died and lost their fluorescence. The results are consistent with the observation of irreversible cessation of root growth at 6 to 8 h of treatment as well as the increase in total length of adventitious roots.

Different Patterns in Accumulation of Specific ROS during Osmotic Stress and Induction of Singlet Oxygen-Sensitive Transcripts after PEG Treatment

As the PEG-induced appearance of singlet oxygen was associated with cell death, we asked if other ROS were associated with cell death in a similar manner. To examine this, the following probes for ROS were employed: BES-So-AM, which was shown to have high selectivity for superoxide (O_2^-) by a nonredox reaction dependent mechanism (Maeda et al., 2005); BES- H_2O_2 , which was shown to be selective for hydrogen peroxide (Maeda et al., 2004); and DAF-FM for nitric oxide (NO; Kojima et al., 1999). The dyes do not provide

quantitative information but indicate the relative and dynamic spatial change. Figure 4A displays the average composite of at least five images during control, early, mid, and late stages of PEG treatment. Figure 4B is a schematic representation of the results in Figure 4A. Cell viability staining by PI is also depicted (Fig. 4, bottom). As shown in Figure 4, each ROS showed strikingly different dynamic accumulation after various PEG treatment durations. Singlet oxygen, as reported by SOSG, was rapidly induced in the epidermal layers, and the signal spread inwards and apically to occupy the whole root. Its presence was detected in cells after their death as well. This suggests that the latter persistent appearance of SOSG fluorescence does not require active cell metabolism and, as noted above, may reflect postmortem degradative processes. The appearance of singlet oxygen broadly recapitulates the change in PI cell permeability (compare top and bottom, Fig. 4, A and B). In contrast to singlet oxygen, NO fluorescence showed constitutive presence at zero time that gradually dissipated in a reciprocal manner to SOSG fluorescence. This may indicate a negative interaction between the two ROS and a requirement for active cell metabolism for NO accumulation. Superoxide was detected constitutively in the epidermal layer and was further induced internally and then dissipated in all tissue. Adversely, hydrogen peroxide appeared in a pervasive burst after the initial stress and slowly dissipated as the tissue died. Notably, all ROS indicators, other than singlet oxygen, required live tissue; however, singlet oxygen was observed in both live and dead cells. The results show that among the ROS types examined, the appearance of singlet oxygen during osmotic stress best overlaps with the dynamics of PEG-induced cell death as measured by changes in cell permeability.

Singlet oxygen is associated with the accumulation of hallmark transcripts in leaves (Mor et al., 2014; Koh and Fluhr, 2016). To establish if the appearance of singlet oxygen in the root as a result of PEG-induced osmotic stress is accompanied by similar diagnostic gene expression patterns, select singlet oxygen- and hydrogen peroxide-associated transcripts were monitored. The specificity of the transcripts was examined by testing their expression in roots following treatment with either photodynamic rose bengal in the light or with hydrogen peroxide. As shown in Figure 5B, each transcript responds only to a specific type of ROS treatment. The application of PEG stimulated the accumulation of both singlet oxygen-specific transcripts and hydrogen peroxide-specific transcripts (Fig. 5A). The results are consistent with the appearance of both these ROS during PEG treatment.

Scavengers of Singlet Oxygen Prevent Cell Death and Promote Root Growth in PEG-Treated Seedlings

As SOSG fluorescence indicated the presence of singlet oxygen both before and after cell death, it is important to consider whether the appearance of singlet oxygen is an essential component of PEG-induced

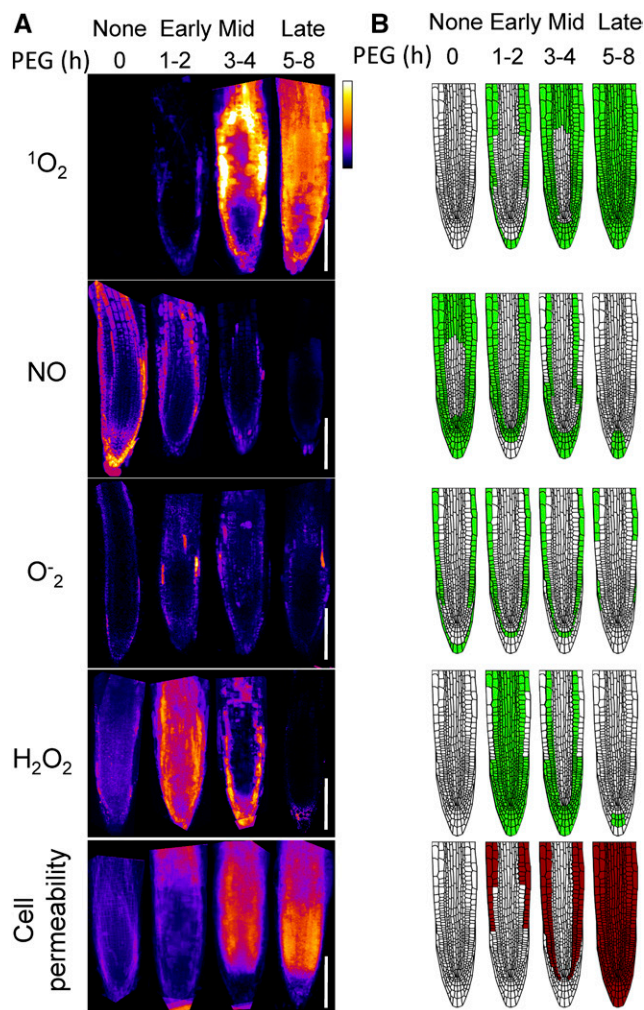


Figure 4. Composite of multiple confocal images of ROS accumulation in root tips exposed to 30% PEG for different durations. A, Composite of confocal images that were collated for each specific signal (ROS probes and propidium iodide stain). Multiple image acquisitions for each time point were aligned manually by rotation and overlaid to create the average composite image using Matlab script. The Look Up Table was set to “Fire” and scaled to maximum as white and minimum as blue. Shown are $^1\text{O}_2$, measured using the SOSG probe; NO, measured using the DAF-FM-AM probe; O_2^- , measured using the Bes-So-AM probe; H_2O_2 , measured using the Bes- H_2O_2 -AC probe, and cell permeability, measured using staining by propidium iodide. B, Schematic representation of the fluorescence shown in A. Scale bar, 100 μm .

stress response or a symptom of cell death. In the former possibility, singlet oxygen would play a direct role in the PEG responses, and specific scavengers of singlet oxygen should mitigate its action. To test this, His, a membrane-permeable specific scavenger of singlet oxygen, was employed. His rapidly forms specific endoperoxides in the presence of singlet oxygen. It is a weaker scavenger of hydroxyl radicals and hydrogen peroxide and does not scavenge superoxide (Matheson et al., 1975; Cai et al., 1995; Ishibashi et al., 1996). The specificity of His as a scavenger for singlet oxygen as

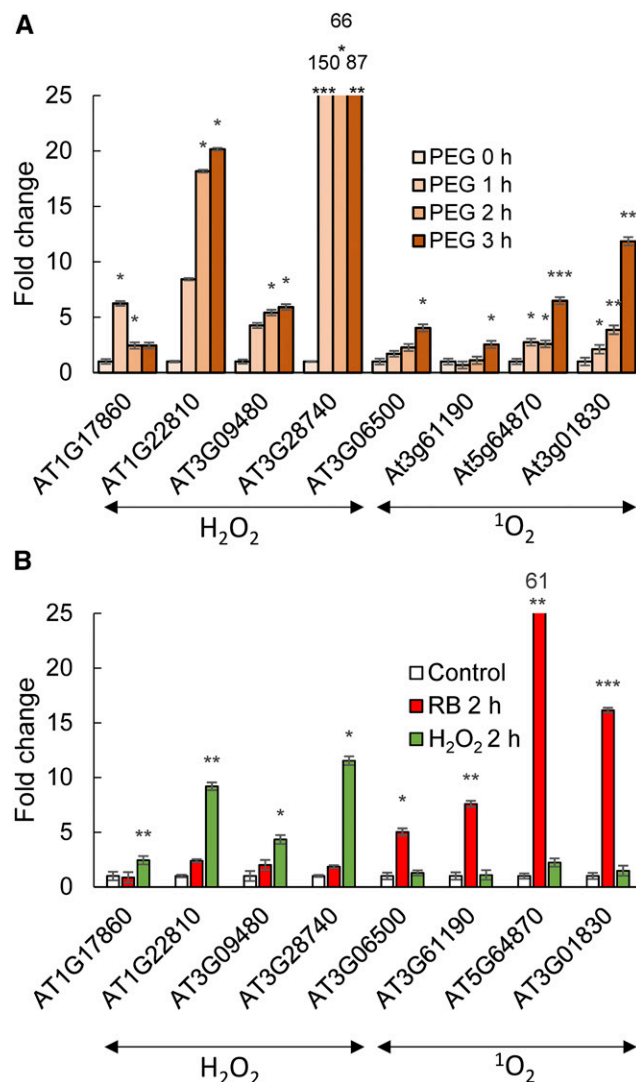


Figure 5. Singlet oxygen- and hydrogen peroxide-specific gene expression in roots. A, Transcript levels were measured by RT-qPCR analysis at 0, 1, 2, and 3 h after treatment with 30% PEG. B, Specificity of gene expression. The transcript level fold change in roots; no treatment (Control); treatment for 2 h in a 100 μM rose bengal aqueous solution under 30 μE light (RB 2 h); treatment for 2 h in a 5 mM H_2O_2 aqueous solution (H_2O_2 2 h). Error bars are SE, $n = 3$. Asterisks indicate significant difference from the untreated sample (Student's t test, $*P < 0.05$, $**P < 0.01$, $***P < 0.001$).

opposed to the other ROS is shown in Supplemental Figure S6. As indicated in Figure 6, A and B, His readily mitigates the appearance of singlet oxygen as measured by SOSG. Significantly, the amount of cell death was reduced by 50% (Fig. 6B) and, as shown in Figure 6C, the presence of His alleviated the repression of the rate of root elongation by PEG. In all, the results lend support for an active role of singlet oxygen in the response to osmotic stress.

The light-independent origin of singlet oxygen is unclear. SHAM is a nonspecific inhibitor of mitochondrial

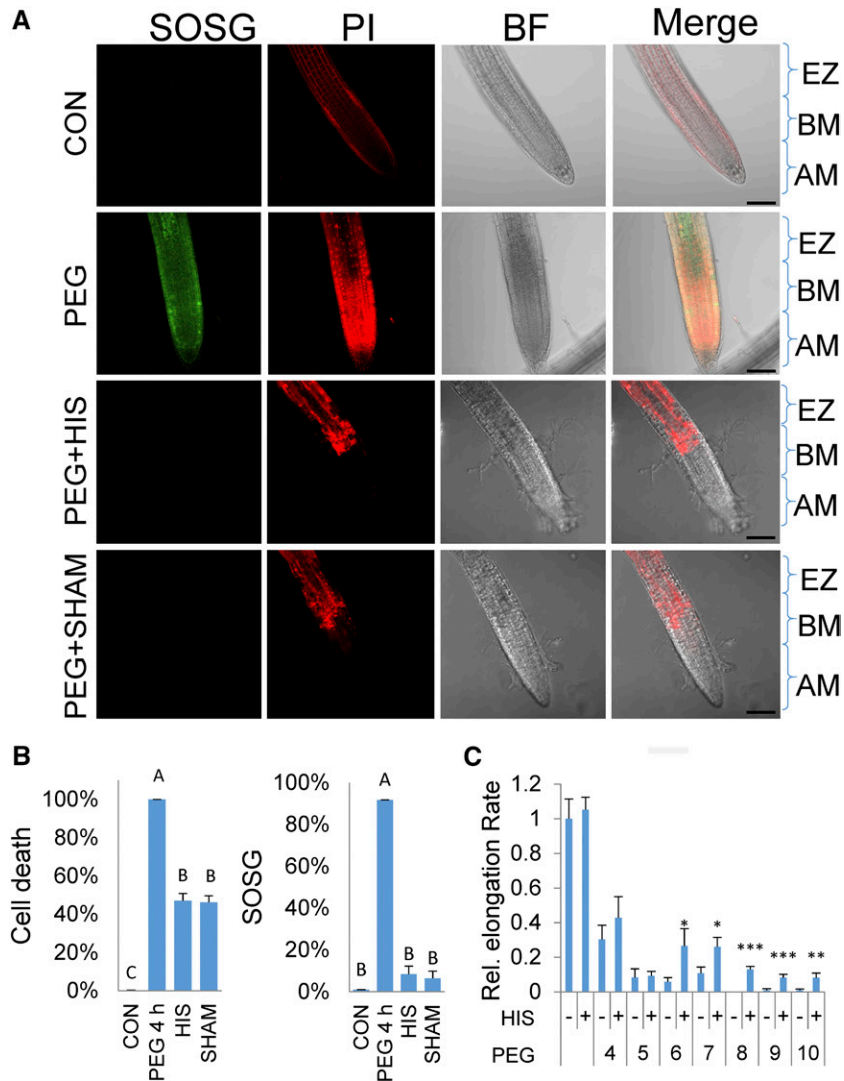


Figure 6. Osmotic shock treatments and the accumulation of singlet oxygen and cell death in the presence of inhibitors and scavengers. A, 7-d-old seedlings were treated with 30% PEG for 4 h and stained with singlet oxygen sensor green (SOSG) and propidium iodide (PI) with or without His (HIS, 5 mM) or salicylhydroxamic acid (SHAM, 1 mM) and viewed with a confocal microscope (see “Materials and Methods”). Confocal laser 561 nm energy settings for the control were set at $Hv = 5$, so that PI staining restricted to the cell walls is clearly visible. All other panels, 561-nm laser was set to $Hv = 2$. Zones indicated are as follows: AM, apical meristem; BM, basal meristem; and EZ, elongation zone. Bar, 100 microns. B, Quantitation of cell death and SOSG fluorescence. Left graph shows cell death as estimated by staining with PI with and without treatments as in A. Right graph shows quantitation of SOSG fluorescence with the treatments as in A. Error bars are SE, $n \geq 8$ seedlings. C, Root elongation rate in seedlings after 30% PEG with or without (+/–) HIS treatment 5 d after exposure to different durations of PEG and His treatments. Asterisks indicate significant difference between PEG and PEG with the addition of His (Student’s *t* test, $*P < 0.05$, $**P < 0.01$, $***P < 0.001$). Error bars are SE, $n \geq 8$.

alternative oxidase enzyme, cyclooxygenases, and lipoxygenases (Peterman and Siedow, 1983). All of these enzymatic activities may produce ROS, including direct or indirect production of singlet oxygen. When applied to seedlings, SHAM inhibited both SOSG fluorescence and cell death (Fig. 6), indicating that singlet oxygen accumulation is sensitive to SHAM, and inhibition of its accumulation likely compromises cell death. SHAM had no effect on probes specific for other ROS (Supplemental Fig. S7). The results suggest

possible sources for singlet oxygen in the root and support an active role for singlet oxygen in promoting the osmotic response.

Vacuolar Collapse Plays a Role in Cell Death and the Response to Osmotic Stress

The dynamic generation of multiple ROS during osmotic stress has been detected here, but based on the use of scavengers and inhibitors, cell death appears to

be associated with the production of singlet oxygen. One method of cellular death is catalyzed by vacuolar disruption (Dickman and Fluhr, 2013), and indeed vacuolar collapse following osmotic stress was visualized by electron microscopy (Duan et al., 2010). A sensitive sensor of vacuolar integrity is the release of cell death inducing protease to the cytoplasm. Serpins are protease inhibitors that are localized to the cytoplasm and are thought to serve a cytoprotective function from vacuolar cell death-inducing proteases. The release of proteases from the vacuole results in the formation of quasi-stable serpin-protease complexes that have been shown to control elicitor-induced cell death (Lampl et al., 2013). To examine if vacuolar collapse may play a role in osmotic stress as well, the relevant transcript levels of the gene encoding the major cell death protease *AtRD21* (AT1G47128) and its cognate serpin *AtSERPIN1* (AT1G47710) were first examined. No significant changes after 3 h were noted for transcript levels of RD21, but a 2-fold increase in *AtSERPIN1* expression was observed (Fig. 7B). This prompted us to use a transgenic line that contains the tagged cytoplasmic AtSERPIN1-HA protease inhibitor, which forms a covalent complex with vacuolar Cys-type cell death proteases upon their release (Lampl et al., 2013; Koh et al., 2016). The line is sensitive to changes in the subcellular distribution of RD21-like proteases that can be monitored by immunoblot analysis. Roots were exposed to PEG, and protein extracts were made in the presence of the protease inhibitor E-64 to prevent the spontaneous formation of additional complexes. The extracts were fractionated on denaturing nonreducing gels to maintain the redox-sensitive covalent bonds. As shown in Figure 7B, upon exposure to PEG for 1 to 6 h, a transient increase in serpin and its complex was observed, indicative of compromised vacuolar integrity. To assess the ramifications of the appearance of serpin-protease complexes, wild-type, overexpression *AtSERPIN1*-HA, and *AtSERPIN1* knockout (*AtSERPIN1*-KO) lines were examined for changes in their sensitivity to osmotic stress. As shown in Figure 7A, *AtSERPIN1*-HA lines showed a protective effect to osmotic stress relative to wild type, as measured by less attenuation of the elongation rate after increasing hours of PEG treatment. Reciprocally, *AtSERPIN1*-KO lines that lack the protective effect of the protease inhibitor exhibited a significant decrease in the elongation rate (Fig. 7A). The results indicate that a component of PEG-induced root cell death is mediated by the vacuole.

DISCUSSION

The use of PEG to alter water potential offers an experimental system to examine components of drought stress (Duan et al., 2010). We showed that, concomitant to the retardation of root elongation and stimulation of auxiliary root growth, both cell death and the production of singlet oxygen can be detected. Cell death was

shown to start at the epidermis and proceed inwards during PEG treatment to affect meristematic tissue. As expected, once the cells of the quiescent center die, the main root ceases to grow and the stimulation of auxiliary root growth reaches its maximum. Interestingly, if osmotic stress ceased before this critical event, the main root continued to grow but was scarred and could not generate root hairs in the affected region. The latter lack of root hairs is consistent with the selective demise of epidermal cells from which root hairs originate and is consistent with root hair developmental plasticity (Grierson et al., 2014). Whereas root hairs are generally thought to aid plants in nutrient acquisition, they also significantly increase the root surface area (Leitner et al., 2010). Hence, their absence in soil area of high osmotic potential may serve to optimize water balance in those places. Interestingly, osmotic stress as applied here did not elicit ROS or cell death response on the more mature sections of root tissue above the elongation zone. Hence, during root maturation, cellular signal transduction pathways that connect osmotic stress to PCD in epidermal cells are lost or undergo vast changes in sensitivity.

ROS are significant secondary messengers of stress signaling. The fluorescence of 2',7'-dichlorofluorescein diacetate, a nonspecific ROS fluorescent probe, was shown previously to increase in PEG-stressed roots (Duan et al., 2010). In this work, we dissected the appearance of various ROS types using a number of highly specific ROS probes, namely singlet oxygen, superoxide, hydrogen peroxide, and nitric oxide. Striking spatial and temporal differences between their accumulation were observed. In all, when ROS appearance was compared with internalization of PI staining serving as an indicator of cell death, the ROS most associated with the dynamics of cell death was singlet oxygen. At different time points after the initiation of osmotic stress, all of the ROS types examined were detected in the apical root meristematic regions and may also play roles in tissue response. However, it is notable that the application of the scavenger His with PEG treatment significantly delayed cell death and reduced the decrease in the rate of elongation. His is specific for singlet oxygen (Telfer, 2014) and, as demonstrated here, did not affect the other ROS. Hence, the appearance of singlet oxygen in the osmotic stress response is not only symptomatic of imminent cellular demise but is also a necessary component.

Singlet oxygen as determined by SOSG fluorescence was shown here to temporally precede cell death and induce transcripts that are specifically sensitive to singlet oxygen generated from photodynamic molecules (Koh et al., 2016). Intriguingly, a fluorescent signal also persisted in dead cells. The persistent signal cannot be due to the residual presence of singlet oxygen as it has an extremely short half-life, but it is likely indicative of ongoing degradative processes that do not require active cellular metabolism. The singlet oxygen-induced response detected here are distinct from the transient bursts of singlet oxygen that have been detected

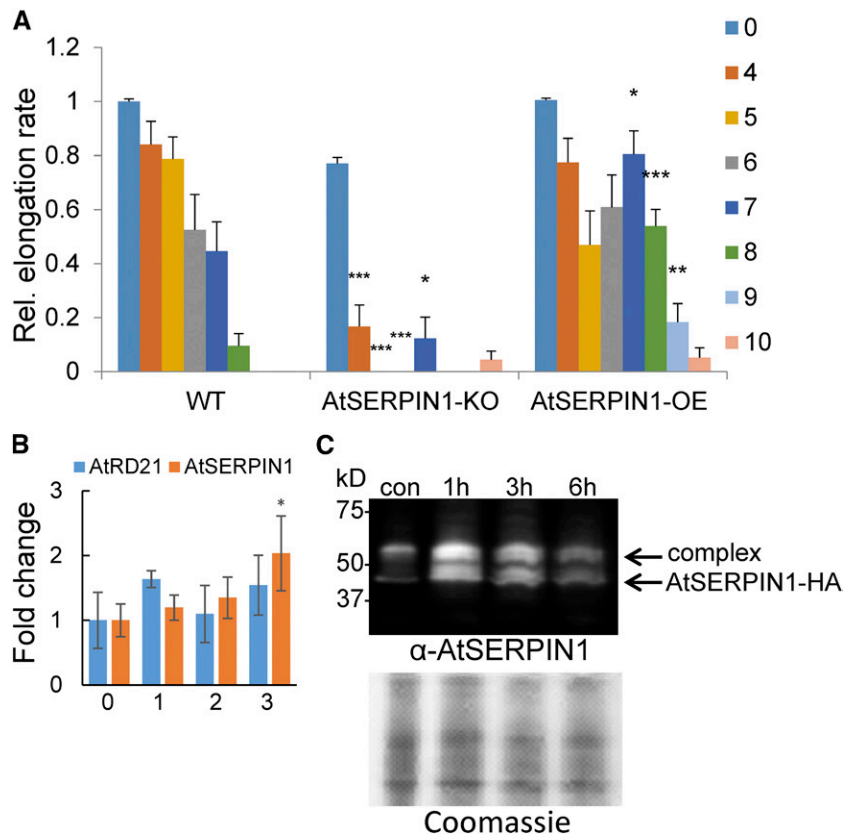


Figure 7. The effect of PEG-induced osmotic shock on mutant *AtSERPIN1* lines. **A**, Quantitation of root elongation rates in wild-type (WT), *AtSERPIN1* knockout (*AtSERPIN1-KO*), and *AtSERPIN1* overexpression (*AtSERPIN1-OE*) lines at 7 d after the 30% PEG treatments indicated on the right (h). Error bars are \pm SE, $n \geq 8$. Asterisks indicate significant difference from the wild-type sample (Student's *t* test, * $P < 0.05$, ** $P < 0.01$, *** $P < 0.001$). **B**, *AtSERPIN1* and *AtRD21* expression levels after PEG treatment. Transcript levels were measured at 0, 1, 2, and 3 h after 30% PEG treatment by RT-qPCR analysis. Error bars are \pm SE, $n = 3$. **C**, Immunoblot analysis of *AtSERPIN1* after nonreducing sodium dodecyl sulfate-polyacrylamide gel electrophoresis fractionation. Immunoblot (top) of *AtSERPIN1* OE roots developed with anti *AtSERPIN1* antibody after the indicated 30% PEG treatments. Bottom, gel stained with Coomassie blue.

previously in root tips of seedlings 1 to 3 min after wounding of the cotyledons (Mor et al., 2014). Those transients were observed in multiple root cell layers and were not associated with cell death. The appearance of systemic wound-induced singlet oxygen transients is thus both spatially and temporally distinct from PEG-induced stress.

The serpin protease inhibitors, including *AtSERPIN1*, act as surveillance monitors of leaked vacuolar proteases (Dickman and Fluhr, 2013; Lampl et al., 2013). Potent vacuolar papain-like Cys proteases are crucial for the turnover of cellular proteins targeted to the vacuole (Gu et al., 2012), and the sequestration of proteases in the vacuole is vital for cell survival. Active proteases that manage to escape their normal transport pathway or that are released from the vacuole during PCD will encounter serpins in the cytoplasm. The stable covalent complexes that are formed dampen activity and delay PCD (Lampl et al., 2013). Seedlings that overexpress the cytoplasmic *AtSERPIN1* were shown here to be less sensitive to osmotic stress and to accumulate

serpin-protease complex. Two scenarios can be envisioned that would result in the formation of such serpin-protease complex during osmotic stress. In the first, vacuoles, as dynamic organelles that respond to osmotic changes, were shown to morph into autophagosome-like vesicles under osmotic stress treatment (Duan et al., 2010). Indeed, analysis of mutants of the autophagic process shows that autophagy plays a role in tolerance to drought stress (Liu et al., 2009). Hence, one consequence of multiple ROS production during osmotic stress would be the accumulation of oxidized proteins that are degraded in the vacuole through autophagy (Xiong et al., 2007). In this scenario, autophagy-directed engulfing of cytoplasmic content by the vacuole may lead to serpin uptake and facilitate the formation of a complex. In another scenario, the formation of a protease-serpin complex would be the direct result of vacuolar collapse that leads to the escape of PCD-inducing proteases to the cytoplasm. Indeed, it was previously shown that singlet oxygen produced by the photodynamic molecule acridine orange caused

vacuolar disruption initiating the release of vacuolar proteases. In that case, the severity of cell death was controlled by the presence of cytoplasmic serpins (Koh et al., 2016). The latter scenario is more consistent with the repressive impact that serpin overexpression exerts on the osmotic stress-induced response shown here.

The source of nonphotosynthetic singlet oxygen can be due to lipoxygenase activity on one of the abundant membrane components, e.g. unsaturated linoleic acid. This activity generates fatty acid hydroperoxides that can interact to form singlet oxygen via the Russell mechanism (Miyamoto et al., 2003, 2007). Alternatively, peroxidation of fatty acid can be the result of a reaction with the perhydroxyl radical, i.e. the protonated form of superoxide or fatty acid reaction with hydroxyl radicals formed between hydrogen peroxide and superoxide in the Haber-Weiss reaction (Haber and Weiss, 1934). However, it is important to keep in mind that elimination of singlet oxygen specifically by the scavenger His was also potent in reducing cell death. Interestingly, wounded leaves were shown to produce singlet oxygen that was diminished in the lipoxygenase mutant *lox2* (Prasad et al., 2017). As shown here, the inhibition of the PEG responses by the reversible inhibitor of lipoxygenase, SHAM, is consistent with this result. The ubiquity of membrane substrate for lipoxygenases can explain the persistence of singlet oxygen production detected here even after cell death. Developmentally programmed singlet oxygen production that correlated with SOSG fluorescence was traced to lipoxygenase activity in grapevine berry skin ripening (Pilati et al., 2014). Indeed, in the case of ripening grape berry, over 10% of the side chains were oxidized to membrane bound 13-peroxy galactolipids. The biological ramifications of direct oxidation could be formation of membrane kinks (Riske et al., 2009). Such kinks may directly contribute to destabilization of the vacuolar membrane that contributes to cell death. Alternatively, membrane destruction is indirect and brought about by a signal transduction mechanism initiated by singlet oxygen. Organelle membrane turnover during osmotic stress detected by Duan et al. (2010) is consistent with the vacuolar membrane leakiness detected here. In this context, it is of interest that in animal tissue active 15-lipoxygenase enzymes were found to be integrated into organelle membranes prior to their permeabilization (van Leyen et al., 1998).

If lipoxygenases are responsible for the production of singlet oxygen, it is an open question how osmotic stress could activate lipoxygenase activity. Some lipoxygenases can be activated by calcium transients (Tatullian et al., 1998), and calcium homeostasis was shown to be perturbed during osmotic stress (Huda et al., 2013). Alternatively, the level of toxic hydroperoxides could be negatively controlled in cells by the rate of their detoxification to less harmful lipid hydroxides through the activities of glutathione peroxidase (GPx) or glutathione transferases (Bao and Williamson, 2000). Indeed, in stressed cells this reaction may be inhibited as was shown for animal cells, where the reduction in

glutathione peroxidase 4 activity led to increased lipid peroxidation and lipoxygenase-dependent cell death (Seiler et al., 2008). Thus, the identification of an exact source for PEG dark-induced singlet oxygen is crucial to our understanding of osmotic stress-induced responses.

MATERIALS AND METHODS

Plant Growth Conditions

Arabidopsis (*Arabidopsis thaliana*; ecotype Columbia-0) seedlings (5 to 7 d old) were grown under white light in a 16-h-light/8-h-dark cycle at 21°C on Murashige and Skoog medium, supplemented with 1% (w/v) Suc and 0.8% (w/v) Phytoagar (Invitrogen). Mutant lines of AtSERPIN1 (Lamp1 et al., 2013) and SCR::GFP lines (Petricka et al., 2012) have been described. For osmotic stress treatment, PEG average molecular weight 8,000 powder (Sigma-Aldrich) was used. For PEG solutions, 30% (w/v) PEG was dissolved in double distilled (dd)H₂O and pH was adjusted to 5.8 using HCl and KOH. Solutions were supplemented with His (5 mM) or salicylhydroxamic acid (0.1 mM) where indicated.

Confocal Microscopy and Image Analysis

All images were taken with a model A1 Confocal Microscope (Nikon). In each figure, the images displayed are of equal laser power and acquisition settings unless indicated. SOSG (Thermo Fisher Scientific) staining was performed by incubation with 100 μM SOSG diluted in ddH₂O in the dark for 20 min and washed three times before staining with 15 μM PI (Thermo Fisher Scientific) in the dark for 30 min. BES-So-AM (Wako Pure Chemical Industries) staining was performed by incubation with 33 μM BES-So-AM diluted in ddH₂O in the dark for 20 min after staining with PI. BES-H₂O₂-AM (10 μM; Wako Pure Chemical Industries) and DAF-FM diacetate (10 μM; Thermo Fisher Scientific) staining was performed by incubation for 1 h after staining with PI. Unless specified, all images were taken at 20× with 1.33 zoom. Excitation of SOSG, BES-So-AM, BES-H₂O₂-AM, and DAF-FM diacetate was at 488 nm, and emission was at 525 nm. For PI staining, excitation was at 561 nm, and emission was at 580 nm. Image analysis was performed using either ImageJ or Nikon NIS-Elements Advanced Research. Statistical analysis was performed using either SAS JMP v8.0 or Microsoft Excel.

RNA Extraction and Reverse Transcription Quantitative PCR Analysis

Three replicates of *Arabidopsis* seedlings (30 to 50 7-d-old seedlings per biological replicate) were used for each treatment. After treatment, the roots and shoots were separated, and RNA was extracted separately from frozen tissues using a standard Trizol extraction method (Sigma-Aldrich). RNA was treated with DNase I (Sigma-Aldrich) and then reverse-transcribed using a high-capacity cDNA reverse transcription kit according to the manufacturer's instructions (Quanta Biosciences). Reverse transcription quantitative-PCR (RT-qPCR) analysis was completed using the SYBR green method (Kapa Biosystems) on a Step One Plus platform (Applied Biosystems) with a standard fast program. RT-qPCR primers were designed using SnapGene software (<http://www.snapgene.com/>) and PrimerBlast (<https://www.ncbi.nlm.nih.gov/tools/primer-blast>). Primers sequences are in Supplemental Table S1.

Gel Fractionation and Immunoblots

Roots were collected from 100 seedlings for each sample. Root proteins were extracted with extraction buffer (20 mM Tris, pH 8.0, 1 mM EDTA, and 50 mM NaCl), and 100 μM E-64 (E-64c; Cayman Chemical) was added to inhibit Cys proteases. Gel fractionation of 30 μg of protein from the extract was carried out on 10% SDS-PAGE. Fractionated proteins were transferred onto polyvinylidene fluoride membrane (Bio-Rad) with a wet transfer for 1.5 h at constant voltage (100 V). The membrane was developed with AtSERPIN1 antibodies (1:1,000) and secondary anti-guinea pig horseradish peroxidase (1:3,000).

Accession Numbers

Sequence data used in this article can be found in the GenBank/EMBL data libraries under the following accession numbers: AT1G17860, NM_101649; AT1G22810, NM_102128; AT3G09480, NM_111782; AT3G28740, NM_113795; AT3G06500, NM_111526; At3g61190, NM_115983; At5g64870, NM_125885; At1g71030, NM_001334485; AT1G47128, NM_103612; and AT1G47710, NM_103664.

Supplemental Data

The following supplemental materials are available.

Supplemental Figure S1. Seven-day-old Arabidopsis seedlings exposed to 30% PEG.

Supplemental Figure S2. Scarred area on root posttreatment with PEG.

Supplemental Figure S3. Differential staining of root tips with propidium iodide without and after PEG treatment.

Supplemental Figure S4. Cell permeability in Arabidopsis roots during PEG-induced water stress.

Supplemental Figure S5. Epidermal tissue treated with PEG for 3 h to illustrate SOSG fluorescence in live and dead cells.

Supplemental Figure S6. Specificity of the inhibition of ROS by His treatment.

Supplemental Figure S7. Specificity of the inhibition of ROS by treatment with salicylhydroxamic acid.

Supplemental Table S1. Primer pairs used in this work.

Received May 23, 2018; accepted June 19, 2018; published June 28, 2018.

LITERATURE CITED

- Bao YP, Williamson G (2000) Selenium-dependent glutathione peroxidases: a highlight of the role of phospholipid hydroperoxide glutathione peroxidase in protection against oxidative damage. *Prog Nat Sci* **10**: 321–330
- Cai Q, Takemura G, Ashraf M (1995) Antioxidative properties of histidine and its effect on myocardial injury during ischemia/reperfusion in isolated rat heart. *J Cardiovasc Pharmacol* **25**: 147–155
- Deak KI, Malamy J (2005) Osmotic regulation of root system architecture. *Plant J* **43**: 17–28
- Dickman MB, Fluhr R (2013) Centrality of host cell death in plant-microbe interactions. *Annu Rev Phytopathol* **51**: 543–570
- Duan Y, Zhang W, Li B, Wang Y, Li K, Sodmergen, Han C, Zhang Y, Li X (2010) An endoplasmic reticulum response pathway mediates programmed cell death of root tip induced by water stress in Arabidopsis. *New Phytol* **186**: 681–695
- Feller U (2016) Drought stress and carbon assimilation in a warming climate: Reversible and irreversible impacts. *J Plant Physiol* **203**: 84–94
- Flors C, Fryer MJ, Waring J, Reeder B, Bechtold U, Mullineaux PM, Nonell S, Wilson MT, Baker NR (2006) Imaging the production of singlet oxygen in vivo using a new fluorescent sensor, Singlet Oxygen Sensor Green. *J Exp Bot* **57**: 1725–1734
- Gechev TS, Dinakar C, Benina M, Toneva V, Bartels D (2012) Molecular mechanisms of desiccation tolerance in resurrection plants. *Cell Mol Life Sci* **69**: 3175–3186
- Giraud E, Ho LHM, Clifton R, Carroll A, Estavillo G, Tan YF, Howell KA, Ivanova A, Pogson BJ, Millar AH, (2008) The absence of ALTERNATIVE OXIDASE1a in Arabidopsis results in acute sensitivity to combined light and drought stress. *Plant Physiol* **147**: 595–610
- Godfray HCJ, Beddington JR, Crute IR, Haddad L, Lawrence D, Muir JE, Pretty J, Robinson S, Thomas SM, Toulmin C (2010) Food security: the challenge of feeding 9 billion people. *Science* **327**: 812–818
- Gollmer A, Arnbjerg J, Blaikie FH, Pedersen BW, Breitenbach T, Daasbjerg K, Glasius M, Ogilby PR (2011) Singlet Oxygen Sensor Green®: photochemical behavior in solution and in a mammalian cell. *Photochem Photobiol* **87**: 671–679
- Grierson C, Nielsen E, Ketelaarc T, Schiefelbein J (2014) Root hairs. *Arabidopsis Book* **12**: e0172

- Gu C, Shabab M, Strasser R, Wolters PJ, Shindo T, Niemer M, Kaschani F, Mach L, van der Hoorn RAL (2012) Post-translational regulation and trafficking of the granulin-containing protease RD21 of *Arabidopsis thaliana*. *PLoS One* **7**: e32422
- Haber F, Weiss J (1934) The catalytic decomposition of hydrogen peroxide by iron salts. *Proc R Soc Lond A Math Phys Sci* **147**: 332–351
- Hara-Nishimura I, Hatsugai N (2011) The role of vacuole in plant cell death. *Cell Death Differ* **18**: 1298–1304
- Hayat S, Hayat Q, Alyemeni MN, Wani AS, Pichtel J, Ahmad A (2012) Role of proline under changing environments: a review. *Plant Signal Behav* **7**: 1456–1466
- Huda KMK, Banu MSA, Garg B, Tula S, Tuteja R, Tuteja N (2013) OsACA6, a P-type IIB Ca²⁺ ATPase promotes salinity and drought stress tolerance in tobacco by ROS scavenging and enhancing the expression of stress-responsive genes. *Plant J* **76**: 997–1015
- Huh GH, Damsz B, Matsumoto TK, Reddy MP, Rus AM, Ibeas JI, Narasimhan ML, Bressan RA, Hasegawa PM (2002) Salt causes ion disequilibrium-induced programmed cell death in yeast and plants. *Plant J* **29**: 649–659
- Ishibashi T, Lee CI, Okabe E (1996) Skeletal sarcoplasmic reticulum dysfunction induced by reactive oxygen intermediates derived from photoactivated rose bengal. *J Pharmacol Exp Ther* **277**: 350–358
- Ji H, Liu L, Li K, Xie Q, Wang Z, Zhao X, Li X (2014) PEG-mediated osmotic stress induces premature differentiation of the root apical meristem and outgrowth of lateral roots in wheat. *J Exp Bot* **65**: 4863–4872
- Joshi R, Shukla A, Sairam RK (2011) *In vitro* screening of rice genotypes for drought tolerance using polyethylene glycol. *Acta Physiol Plant* **33**: 2209–2217
- Koh E, Fluhr R (2016) Singlet oxygen detection in biological systems: Uses and limitations. *Plant Signal Behav* **11**: e1192742
- Koh E, Carmieli R, Mor A, Fluhr R (2016) Singlet oxygen-induced membrane disruption and serpin-protease balance in vacuolar-driven cell death. *Plant Physiol* **171**: 1616–1625
- Kojima H, Urano Y, Kikuchi K, Higuchi T, Hirata Y, Nagano T (1999) Fluorescent indicators for imaging nitric oxide production. *Angew Chem Int Ed Engl* **38**: 3209–3212
- Lagerwerff JV, Ogata G, Eagle HE (1961) Control of osmotic pressure of culture solutions with polyethylene glycol. *Science* **133**: 1486–1487
- Lamp N, Budai-Hadrian O, Davydov O, Joss TV, Harrop SJ, Curmi PMG, Roberts TH, Fluhr R (2010) *Arabidopsis* AtSerpin1, crystal structure and in vivo interaction with its target protease RESPONSIVE TO DESICCATION-21 (RD21). *J Biol Chem* **285**: 13550–13560
- Lamp N, Alkan N, Davydov O, Fluhr R (2013) Set-point control of RD21 protease activity by AtSerpin1 controls cell death in Arabidopsis. *Plant J* **74**: 498–510
- Lee S, Seo PJ, Lee HJ, Park CM (2012) A NAC transcription factor NTL4 promotes reactive oxygen species production during drought-induced leaf senescence in Arabidopsis. *Plant J* **70**: 831–844
- Leitner D, Klepsch S, Ptashnyk M, Marchant A, Kirk GJD, Schnepf A, Roose T (2010) A dynamic model of nutrient uptake by root hairs. *New Phytol* **185**: 792–802
- Liu Y, Xiong Y, Bassham DC (2009) Autophagy is required for tolerance of drought and salt stress in plants. *Autophagy* **5**: 954–963
- Maeda H, Fukuyasu Y, Yoshida S, Fukuda M, Saeki K, Matsuno H, Yamauchi Y, Yoshida K, Hirata K, Miyamoto K (2004) Fluorescent probes for hydrogen peroxide based on a non-oxidative mechanism. *Angew Chem Int Ed Engl* **43**: 2389–2391
- Maeda H, Yamamoto K, Nomura Y, Kohno I, Hafsli L, Ueda N, Yoshida S, Fukuda M, Fukuyasu Y, Yamauchi Y, (2005) A design of fluorescent probes for superoxide based on a nonredox mechanism. *J Am Chem Soc* **127**: 68–69
- Matheson IBC, Etheridge RD, Kratowich NR, Lee J (1975) The quenching of singlet oxygen by amino acids and proteins. *Photochem Photobiol* **21**: 165–171
- Miller G, Suzuki N, Ciftci-Yilmaz S, Mittler R (2010) Reactive oxygen species homeostasis and signalling during drought and salinity stresses. *Plant Cell Environ* **33**: 453–467
- Miyamoto S, Martinez GR, Medeiros MHG, Di Mascio P (2003) Singlet molecular oxygen generated from lipid hydroperoxides by the russell mechanism: studies using ¹⁸O-labeled linoleic acid hydroperoxide and monomol light emission measurements. *J Am Chem Soc* **125**: 6172–6179
- Miyamoto S, Ronsein GE, Prado FM, Uemi M, Corrêa TC, Toma IN, Bertolucci A, Oliveira MCB, Motta FD, Medeiros MHG, (2007) Biological

- hydroperoxides and singlet molecular oxygen generation. *IUBMB Life* **59**: 322–331
- Monetti E, Kadono T, Tran D, Azzarello E, Arbelet-Bonin D, Biligui B, Briand J, Kawano T, Mancuso S, Bouteau F** (2014) Deciphering early events involved in hyperosmotic stress-induced programmed cell death in tobacco BY-2 cells. *J Exp Bot* **65**: 1361–1375
- Mor A, Koh E, Weiner L, Rosenwasser S, Sibony-Benyamini H, Fluhr R** (2014) Singlet oxygen signatures are detected independent of light or chloroplasts in response to multiple stresses. *Plant Physiol* **165**: 249–261
- Munne-Bosch S, Alegre L** (2004) Die and let live: leaf senescence contributes to plant survival under drought stress. *Funct Plant Biol* **31**: 203–216
- Patade VY, Bhargava S, Suprasanna P** (2012) Transcript expression profiling of stress responsive genes in response to short-term salt or PEG stress in sugarcane leaves. *Mol Biol Rep* **39**: 3311–3318
- Peterman TK, Siedow JN** (1983) Structural features required for inhibition of soybean lipoxygenase-2 by propyl gallate: evidence that lipoxygenase activity is distinct from the alternative pathway. *Plant Physiol* **71**: 55–58
- Petricka JJ, Schauer MA, Megraw M, Breakfield NW, Thompson JW, Georgiev S, Soderblom EJ, Ohler U, Moseley MA, Grossniklaus U** (2012) The protein expression landscape of the *Arabidopsis* root. *Proc Natl Acad Sci USA* **109**: 6811–6818
- Petrov V, Hille J, Mueller-Roeber B, Gechev TS** (2015) ROS-mediated abiotic stress-induced programmed cell death in plants. *Front Plant Sci* **6**: 69
- Pilati S, Brazzale D, Guella G, Milli A, Ruberti C, Biasioli F, Zottini M, Moser C** (2014) The onset of grapevine berry ripening is characterized by ROS accumulation and lipoxygenase-mediated membrane peroxidation in the skin. *BMC Plant Biol* **14**: 87
- Prasad A, Sedlářová M, Kale RS, Pospíšil P** (2017) Lipoxygenase in singlet oxygen generation as a response to wounding: in vivo imaging in *Arabidopsis thaliana*. *Sci Rep* **7**: 9831
- Rhoads DM, Umbach AL, Subbaiah CC, Siedow JN** (2006) Mitochondrial reactive oxygen species. Contribution to oxidative stress and interorganellar signaling. *Plant Physiol* **141**: 357–366
- Riske KA, Sudbrack TP, Archilha NL, Uchoa AF, Schroder AP, Marques CM, Baptista MS, Itri R** (2009) Giant vesicles under oxidative stress induced by a membrane-anchored photosensitizer. *Biophys J* **97**: 1362–1370
- Rogers H, Munné-Bosch S** (2016) Production and scavenging of reactive oxygen species and redox signaling during leaf and flower senescence: similar but different. *Plant Physiol* **171**: 1560–1568
- Rosenwasser S, Fluhr R, Joshi JR, Leviatan N, Sela N, Hetzroni A, Friedman H** (2013) ROSMETER: a bioinformatic tool for the identification of transcriptomic imprints related to reactive oxygen species type and origin provides new insights into stress responses. *Plant Physiol* **163**: 1071–1083
- Sabatini S, Heidstra R, Wildwater M, Scheres B** (2003) SCARECROW is involved in positioning the stem cell niche in the *Arabidopsis* root meristem. *Genes Dev* **17**: 354–358
- Seiler A, Schneider M, Förster H, Roth S, Wirth EK, Culmsee C, Plesnila N, Kremmer E, Rådmark O, Wurst W** (2008) Glutathione peroxidase 4 senses and translates oxidative stress into 12/15-lipoxygenase dependent- and AIF-mediated cell death. *Cell Metab* **8**: 237–248
- Takasaki H, Maruyama K, Takahashi F, Fujita M, Yoshida T, Nakashima K, Myouga F, Toyooka K, Yamaguchi-Shinozaki K, Shinozaki K** (2015) SNAC-As, stress-responsive NAC transcription factors, mediate ABA-inducible leaf senescence. *Plant J* **84**: 1114–1123
- Tatulian SA, Steczko J, Minor W** (1998) Uncovering a calcium-regulated membrane-binding mechanism for soybean lipoxygenase-1. *Biochemistry* **37**: 15481–15490
- Telfer A** (2014) Singlet oxygen production by PSII under light stress: mechanism, detection and the protective role of β -carotene. *Plant Cell Physiol* **55**: 1216–1223
- van der Weele CM, Spollen WG, Sharp RE, Baskin TI** (2000) Growth of *Arabidopsis thaliana* seedlings under water deficit studied by control of water potential in nutrient-agar media. *J Exp Bot* **51**: 1555–1562
- van Leyen K, Duvoisin RM, Engelhardt H, Wiedmann M** (1998) A function for lipoxygenase in programmed organelle degradation. *Nature* **395**: 392–395
- Verslues PE, Ober ES, Sharp RE** (1998) Root growth and oxygen relations at low water potentials. Impact Of oxygen availability in polyethylene glycol solutions. *Plant Physiol* **116**: 1403–1412
- Voss I, Sunil B, Scheibe R, Raghavendra AS** (2013) Emerging concept for the role of photorespiration as an important part of abiotic stress response. *Plant Biol (Stuttg)* **15**: 713–722
- Xiong Y, Contento AL, Nguyen PQ, Bassham DC** (2007) Degradation of oxidized proteins by autophagy during oxidative stress in *Arabidopsis*. *Plant Physiol* **143**: 291–299